Society For Biomaterials

Crosslinking of poly(L-lactide) nanofibers with triallyl isocyanutrate by gamma-irradiation for tissue engineering application

Chuanglong He,[1,2] Wei Feng,[2] Lijun Cao,[2] Linpeng Fan[2]

[1]State Key Laboratory for Modification of Chemical Fibers and Polymer Materials, Donghua University, Shanghai 201620, People's Republic of China
[2]College of Chemistry, Chemical Engineering and Biotechnology, Donghua University, Shanghai 201620, People's Republic of China

Received 19 May 2011; revised 2 July 2011; accepted 15 August 2011
Published online 27 September 2011 in Wiley Online Library (wileyonlinelibrary.com). DOI: 10.1002/jbm.a.33235

Abstract: The radiation crosslinked poly(L-lactide) (PLLA) electrospun nanofibers have been developed with improved thermal stability and mechanical properties. Trially isocyanurate (TAIC) were added into PLLA solution at different weight ratios (1, 3, and 5%) and electrospun into nanofibrous mats, the mats were then irradiated by gamma ray at different radiation doses (5, 10, and 25 kGy) to crosslink the PLLA chains. Their surface morphology, thermal properties, mechanical properties, and biodegradation properties were investigated and compared before and after gamma irradiation. Furthermore, the *in vitro* biocompatibilities were also evaluated by using mouse L929 fibroblasts. The results indicated that the efficient crosslinking networks can be generated when the TAIC content is higher than 3%. The thermal stability and tensile mechanical properties were significantly increased at higher irradiation dose of 10 and 25 kGy. However, radiation dose at 25 kGy have an adverse effect on the thermal stability of crosslinked samples due to thermal degradation induced by irradiation, the crosslinked samples irradiated at 10 kGy exhibited the best enzymatic degradation. The *in vitro* results also revealed that the crosslinked PLLA/TAIC composite nanofibers did not induce cytotoxic effects and are suitable for cell growth. Therefore, the crosslinked PLLA nanofibers are one of the promising materials for future tissue engineering applications. © 2011 Wiley Periodicals, Inc. J Biomed Mater Res Part A: 99A: 655–665, 2011.

Key Words: poly(L-lactide), electrospun nanofibers, crosslinking, triallyl isocyanutrate, gamma-irradiation

How to cite this article: He C, Feng W, Cao L, Fan L. 2011. Crosslinking of poly(L-lactide) nanofibers with triallyl isocyanutrate by gamma-irradiation for tissue engineering application. J Biomed Mater Res Part A 2011:99A:655–665.

INTRODUCTION

Tissue engineering has emerged as a promising approach to repair, replace, or regenerate diseased or damaged tissues and organs without the limitations of traditional therapies.[1] In this approach, the scaffolding material serves as a mimic for the native extracellular matrix (ECM) and plays an important role in successful tissue regeneration by providing structural support and biological signals for cellular growth and tissue formation. Hence, it is desirable that scaffold enables to mimic the natural ECM in structure and function.[2,3] To achieve this goal, a number of nanofibrous scaffolds have been developed to mimic the nanoscale structure of native fibrillar collagen, which can be produced by means of three main techniques including self-assembly, phase separation, and electrospinning.[4–6] Nanofibrous scaffolds produced using these techniques provide the combined characteristics of small fiber diameter, appropriate porosity, and high surface area-to-volume ratio, making them very effective for functional tissue engineering.[5,7]

Poly(L-lactide) (PLLA) is a biodegradable, biocompatible, and nontoxic polyester, which can be fabricated into nanofibrous mats or scaffolds by either electrospinning or phase separation.[8,9] PLLA nanofibers have attracted considerable attentions recently as one of the most promising materials for extensive biomedical applications such as wound closure materials, tissue engineering scaffolds, and drug delivery carriers.[9–11] However, poor heat stability and mechanical properties of PLLA-based materials restrict their applications as ordinary structural material.[12–14] Many attempts have been made to improve the heat stability and mechanical properties of PLLA-based materials over the past years.[12,14,15] Among them, the introduction of crosslinking structure between PLLA molecules by some chemical and physical treatments has been proved to be an effective way

Correspondence to: C. He; e-mail: hcl@dhu.edu.cn
Contract grant sponsor: Natural Science Foundation of Shanghai; contract grant number: 11ZR1400100
Contract grant sponsor: Shanghai BaiYuLan Science and Technology Foundation; contract grant number: 2010B001
Contract grant sponsor: Doctoral Fund of Ministry of Education of China; contract grant number: 200802551014
Contract grant sponsor: Fundamental Research Funds for the Central Universities, Open Foundation of State Key Laboratory for Modification of Chemical Fibers and Polymer Materials; contract grant number: LK0804
Contract grant sponsor: Program of Introducing Talents of Discipline to Universities; contract grant number: B07024

to improve their heat stability and biodegradation rate.[14,16] In general, the crosslinking structure can be effectively formed by gamma or electron beam irradiation of PLLA containing suitable concentration of various crosslinking agents such as trially isocyanurate (TAIC). TAIC has three functional groups and a cyclic unit in its structure, so it has been proposed as one of the most effective crosslinking agents for PLLA. Previous studies[13,16,17] have mainly focused on the effects of the crosslinking parameters on the properties of PLLA bulk materials such as films and moldings. Hitherto, only few studies have been conducted to explore the radiation-induced crosslinking of PLLA nanofibers and their biocompatibility for potential tissue engineering applications.

The aim of present study is therefore to examine the effects of irradiation-induced crosslinking on the physicochemical properties and biocompatibility of electrospun PLLA nanofibers. The PLLA/TAIC electrospun nanofibers with different TAIC contents were fabricated and then crosslinked by gamma radiation at different doses. The thermal and mechanical properties of these crosslinked PLLA nanofibers were investigated through the TAIC content and radiation dose. Moreover, the enzymatic degradation properties and *in vitro* biocompatibility of crosslinked nanofibers were also evaluated by using proteinase K and L929 mouse fibroblasts respectively for potential tissue engineering applications.

MATERIALS AND METHODS

Materials

PLLA with a weight-average molecular weight (M_w) of 247,000 g mol^{-1} was purchased from Daigang Biomaterials (Jinan, China) and was used as received. Triallyl isocyanutrate (TAIC) and Proteinase K (activity: 30 U mg^{-1}) were purchased from Sigma-Aldrich (Shanghai, China). Sodium azide was purchased from J&K Chemical (Beijing, China). Other reagents were bought from Sinopharm Chemical Reagent (Shanghai, China). Mouse fibroblasts (L929) were obtained from Institute of Biochemistry and Cell Biology (Chinese Academy of Sciences, China). All culture media and reagents were purchased from Gibco BRL Life Technologies (USA).

Fabrication of electrospun nanofibers and irradiations

For nanofibers fabrication, PLLA pellets were first dissolved in a mixture of dichloromethane and acetone with a volume ratio of 2:1. After complete dissolution, specific weight ratios (1, 3, and 5%) of TAIC were added and stirred until the mixture became homogeneous. The concentration of resultant solutions was kept at 10 wt %. The solutions were separately placed in a 10-mL plastic syringe fitted with an 18 gauge needle. The electrospinning were performed at 18 kV by using a high-voltage supply (BGG6-358, BMEI, China). A plate of aluminum foil was grounded and placed 15 cm below the needle tip, and used to collect nanofibers. The solution was fed into the needle using a syringe pump (789100C, Cole-Parmer Instruments, USA) at a flow rate of 3 mL h^{-1}. The prepared fibrous mats with thickness of around 0.2 mm were dried in a vacuum oven for 48 h to remove the residual solvents. The film samples were sealed in polypropylene bag and irradiated at room temperature in a 2.22×10^{15} Bq ^{60}Co gamma-ray source at different radiation doses (5, 10, and 25 kGy) with 50 Gy min^{-1} irradiation dose rate. The obtained samples were then stored at room temperature in a desiccator for further measurements.

Characterization of the fibrous scaffolds

Morphology observation. Scanning electron microscopy (SEM) images of PLLA/TAIC composite fibers before and after irradiation were obtained with a Hitachi S-2700 scanning electron microscope (Hitachi, Japan) at an accelerating voltage of 10 kV. Prior to SEM observation, all of the specimens were sputter coated with gold for 60 s. The diameters of nanofibers were measured based on SEM images using image visualization software (ImageJ 1.34s, NIH Image, USA). The average fiber diameter and its distribution were determined from about 100 measurements on a typical SEM image.

Attenuated total reflectance-Fourier transform infrared spectra (ATR-FTIR). ATR-FTIR spectra were obtained with a Nicolet-670 FTIR spectroscopy (Nicolet-Thermo, USA). The infrared spectra of the samples were measured over a wavelength range of 4000–500 cm^{-1} with a resolution of 4 cm^{-1}.

Thermal analysis. The thermal properties of samples (ca. 4 mg) were measured by DSC-204 F1 (Netzsch, Germany) thermal analysis instrument using aluminum oxide as the standard. The samples were measured from 25 to 200°C under nitrogen gas at a heating rate of 10°C min^{-1}.

The thermal stability of samples was investigated with a TG-209 F1 thermal analyzer (Netzsch, Germany), about 3–4 mg sample was used in an aluminum pan and heated at a rate of 10°C min^{-1} from ambient temperature to 500°C in a nitrogen gas atmosphere. The nitrogen gas flow rate was 40 mL min^{-1}.

Mechanical properties. The samples for tensile test were prepared according to our previous study.[18] A straight-line sample with a planar area of 50 mm × 10 mm was cut from the PLLA sample, each end of which was glued in between two pieces of 10 mm × 10 mm tapes, leaving a gauge length of 30 mm. The tensile testing was performed using a universal materials tester (H5 K-S, Hounsfield , UK) with a 50-N load cell at ambient temperature 25°C and humidity 65%. A cross-head speed of 10 mm min^{-1} was used for all the specimens. For each group, at least five specimens were tested to calculate the mean value and standard deviation.

Dynamic mechanical analyses. Dynamic mechanical properties were investigated using a dynamic mechanical analyzer DMA Q800 (TA instruments, USA). The sample dimensions were 20 × 10 × 0.2 mm^3. The film was measured under the tensile at a constant frequency of 1.0 Hz,

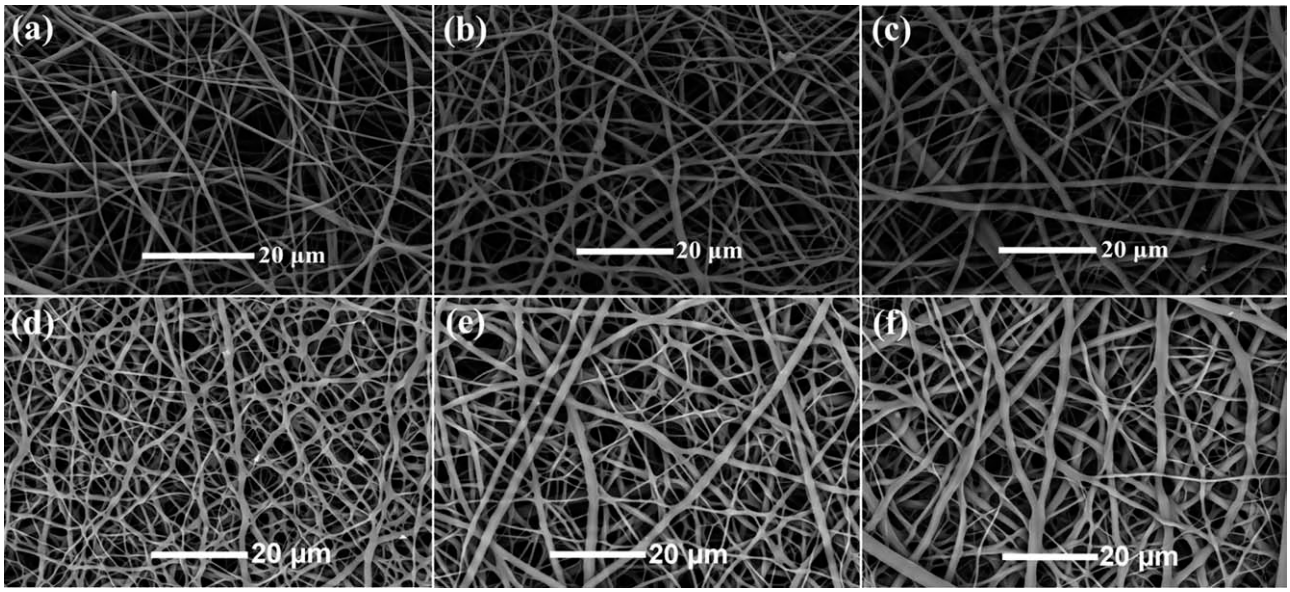

FIGURE 1. SEM images of PLLA/TAIC nanofibers with various concentration of TAIC before gamma irradiation: (a) 1%, (b) 3%, (c) 5%, and after irradiation at 25 kGy: (d) 1%, (e) 3%, (f) 5%.

temperature ranging from 25 to 200°C and a heating rate of 2°C min^{-1} under nitrogen gas flow.

Enzymatic degradation. The enzymatic degradation behavior was evaluated from the morphological change and mass loss. The weighted film samples (10 × 10 mm^2 dimension) were placed in 15-mL centrifuge tubes with 5 mL of 0.1 mol L^{-1} Tris/HCl buffer (pH 8.6) containing 0.25 mg of proteinase K and 1.0 mg of sodium azide, the tubes were subsequently placed inside an orbital incubator a 37°C, rotating at 60 rpm, for up to 8 days. At predetermined intervals, triplicate specimens for each sample condition were taken out of solutions and washed with distilled water, methanol and freeze-dried to a constant weight in vacuum. Biodegradation was evaluated by measuring weight loss values (mg) per unit area (cm^2) of the film samples. The morphological change was also estimated from SEM observation as above. For comparison, blank test (neat PLLA film) was carried out using the same buffer solution without enzyme.

Biological testing

Cell culture and scaffold preparation. The thawed L929 mouse fibroblasts were cultured in a 5% CO_2, humid atmosphere at 37°C in Dulbecco's modified Eagle's medium (DMEM) containing 10% fetal bovine serum, 100 U mL^{-1} penicillin and 100 U mL^{-1} streptomycin, the culture medium was changed every other day.

Prior to cell seeding, the fibrous films were cut into round shape pieces with a 15 mm diameter. The samples were fixed in the 24-well plate with stainless steel rings and sterilized with 75% alcohol solution for 4 h, washed three times with phosphate-buffered saline solution (PBS) for 30 min each, and twice with cell culture medium for 1 h each.

Cell viability evaluation. For proliferation study, L929 mouse fibroblasts (5 × 10^4 mL^{-1}) were seeded on the scaffolds with neat PLLA scaffold as control. The proliferation of the cells on each specimen was determined after varying culture period of 1, 3, 5, and 7 days, respectively. The viability of the cells was quantified by 3-[4, 5-dimethylthiazol-2-yl]-2, 5-diphenyltetrazolium bromide (MTT) assay at the absorbance of 570 nm using an enzyme-labeled instrument (MK3, Thermo, USA). Morphological appearance of the cells after 3 days of culture was observed by SEM (Hitachi S-2700, Japan). Cells cultured on scaffolds were washed with PBS and then fixed with 4% glutaraldehyde overnight at 4°C. The samples were dehydrated in 50, 75, and 100% alcohol solutions and dried under vacuum. Afterwards, the samples were sputter coated with gold and examined using a SEM at voltage of 15 kV.

Statistical analysis

All experiments were conducted at least three times and all values were reported as the mean and standard deviation. Statistical analysis was carried out by the one-way analysis of variance (one-way ANOVA) and Scheffe's post hoc test in SPSS (SPSS). The statistical difference between two sets of data was considered when $p < 0.05$.

RESULTS AND DISCUSSION

Structure and appearance of nanofibrous scaffolds

Figure 1 shows the typical SEM images of PLLA/TAIC nanofibers with various concentration of TAIC before and after gamma irradiation at 25 kGy. All the scaffolds showed a porous morphology with random aligned fibers, but the crosslinked scaffolds [Fig. 1(d–f)] exhibited more compact fibrous structure and relatively rougher surface morphology as compare to uncrosslinked counterparts [Fig. 1(a–c)]. The average fiber diameters of all the PLLA/TAIC scaffolds

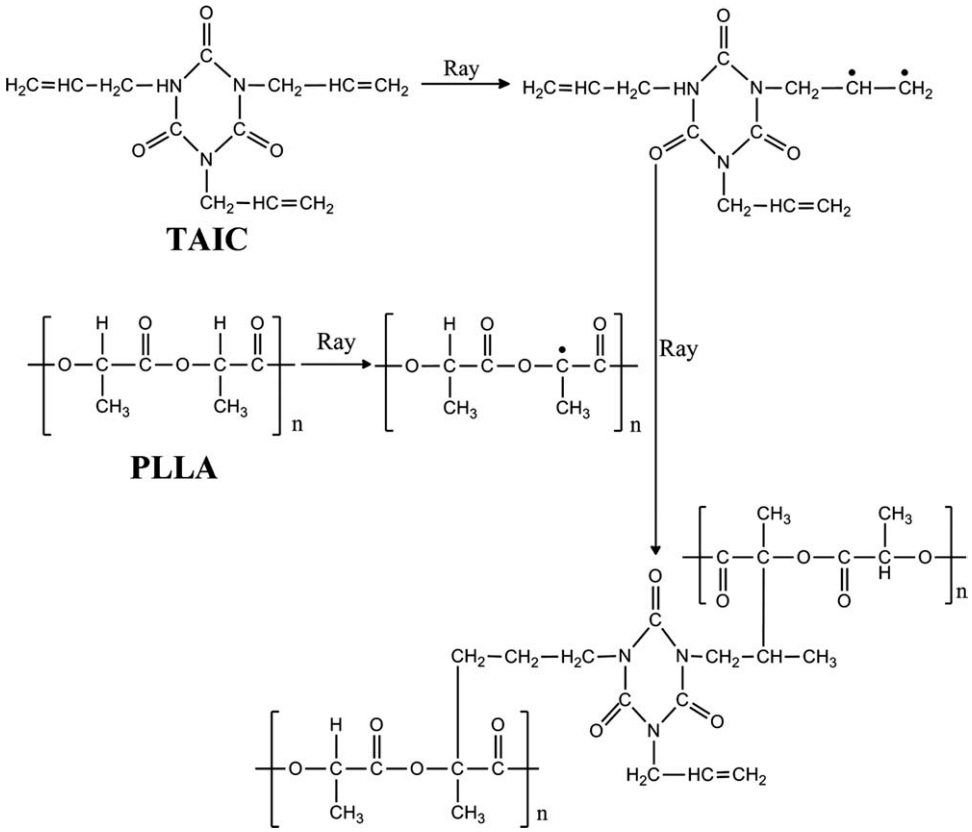

FIGURE 2. Possible radiation-induced crosslinking of TAIC between two PLLA molecules (the third allyl group in TAIC was not activated).

increased with the increasing of TAIC content in scaffolds. The radiation crosslinking results in only relatively small changes in the average fiber diameters. For example, the fiber diameters for uncrosslinked scaffolds containing TAIC of 1, 3, and 5% were 705 ± 234, 919 ± 269, and 1026 ± 391 nm, respectively, whereas these values changed to 668 ± 250, 868 ± 399, and 1058 ± 566 nm, respectively, after irradiation at 25 kGy. The results revealed that the content of TAIC had a notable effect on the diameters of the obtained nanofibers. This can be explained by the increase of solution viscosity at high TAIC content due to interactions between TAIC and PLLA molecules. In general, a high viscosity results in a large fiber diameter during electrospinning process.[19]

The electrospinning process usually tends to produce a loose and scraggly fibrous structure on the surface of the substrate due to the mutual electrostatic repulsion among the resulting nanofibers.[10] TAIC has been proved to be one of the most effective crosslinking agents for PLLA. When PLLA/TAIC composite nanofibers were irradiated by gamma rays or electron beams, Hydrogen atom abstraction occurred predominantly from the methine groups in PLLA chains.[14,20] At the same time, the double bonds of allyl groups in TAIC were broken to form a pair of radicals ($-\dot{C}H-\dot{C}H_2$) and subsequently combined with the polymer radicals. According to Mitomo et al.,[14] $-\dot{C}H-\dot{C}H_2$ group in TAIC may recombine with abstracted $\dot{H}$ to form $-\dot{C}H-CH_3$ or $-CH_2-\dot{C}H_2$, both remnant radicals subsequently combine with PLLA to produce two kinds of combinations that usually occurred at the radiation-induced crosslinking, as shown in Figure 2. Thus, a compact crosslinking network with effective crosslinking points can be formed between PLLA and TAIC molecules,[13,14,20] which makes a slight decrease in fiber diameter [Fig. 1(d,e)]. The molecular structure of TAIC and a schematic drawing of radiation-induced crosslinking with the presence of TAIC are depicted in Figure 3.

FTIR analysis

Figure 4 shows the FTIR spectra of the neat PLLA nanofibers and crosslinked PLLA/TAIC nanofibers with various concentration of TAIC irradiated at 25 kGy. The peaks at about 1757 and 1188 cm^{-1} which belong to the C=O stretching and C—O—C stretching of PLLA, respectively, are clearly visible in all the spectra.

After the chemical reaction with TAIC, one new peak appears at about 1694 cm^{-1} (C=O of TAIC), which can be observed in the spectra of crosslinked PLLA. The intensities of this new peak increase with increasing TAIC content, which clearly confirms the chemical crosslinking reaction between PLLA and TAIC.

Thermal properties

DSC thermograms of crosslinked PLLA with different TAIC contents and different radiation doses are shown in Figure 5. Figure 5(a) shows DSC heating curves of the crosslinked PLLA/TAIC fibrous scaffolds containing different TAIC

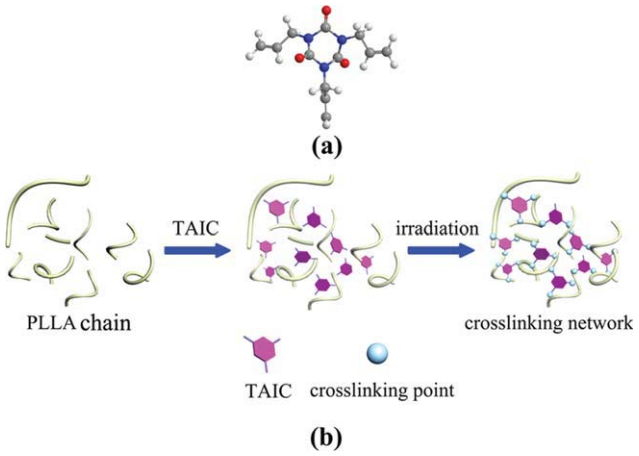

FIGURE 3. (a) Molecular structure of TAIC. (b) Schematic drawing of radiation-induced crosslinking with the presence of TAIC. [Color figure can be viewed in the online issue, which is available at wileyonlinelibrary.com.]

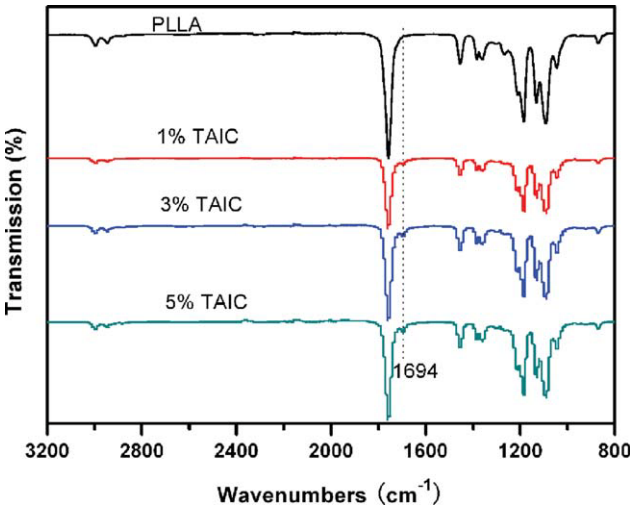

FIGURE 4. FTIR spectra of the neat PLLA nanofibers and crosslinked PLLA/TAIC nanofibers with various concentration of TAIC irradiated at 25 kGy. [Color figure can be viewed in the online issue, which is available at wileyonlinelibrary.com.]

contents irradiated at 25 kGy. DSC curve of neat PLLA fibers reveals three major peaks at temperatures corresponding to the glass transition temperature (T_g), cold crystallization temperature (T_{cc}), and melting temperature (T_m). For PLLA/TAIC crosslinked samples, only one endothermic peak at about 180°C can be clearly discerned, which corresponds to the T_m of single crystal in two different phases. In addition, the melting temperature of crosslinked samples decreased with increasing the TAIC content, whereas the crystallization peak of highly crosslinked PLLA/3% TAIC and PLLA/5% TAIC samples disappeared entirely. These results indicated that the efficient crosslinking networks could be generated in the crosslinked samples when the TAIC content is higher than 3%, and this crosslinking network inhibited the segmental motion for crystallization. These results are in good agreement with those of previous studies on radiation-induced crosslinking of PLLA.[16,17]

Figure 5(b) shows the DSC curves of PLLA/3% TAIC crosslinked at different radiation doses. The glass-transition, cold crystallization and melting peaks can be clearly observed in the curve of unirradiated sample, but the crystallization peak disappeared in the curves of irradiated samples, and the melting temperatures slightly reduced with the increasing of radiation dose. The result confirmed that irradiation by gamma ray is a most important factor in the crosslinking of PLLA with TAIC. The crosslinking structure can be formed even in the lower radiation dose of 5 kGy, and the higher crosslinking density can be achieved at high radiation dose. The disappearance of crystallization peaks in

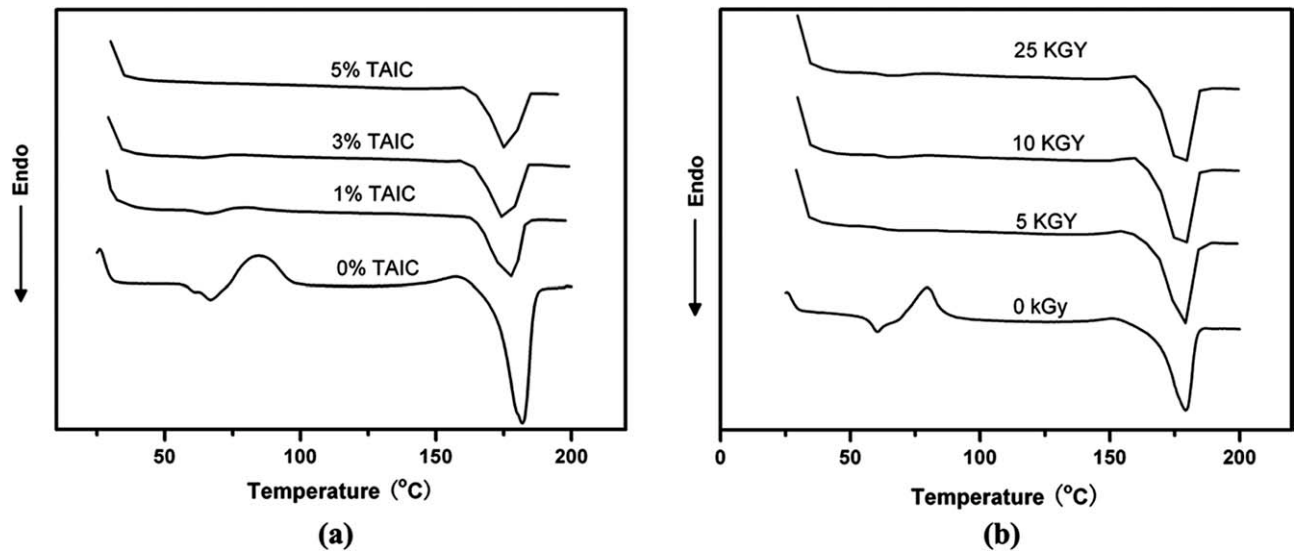

FIGURE 5. DSC heating curves of (a) PLLA/TAIC nanofibers containing different TAIC contents irradiated at 25 kGy. (b) PLLA/3% TAIC nanofibers crosslinked at different radiation doses.

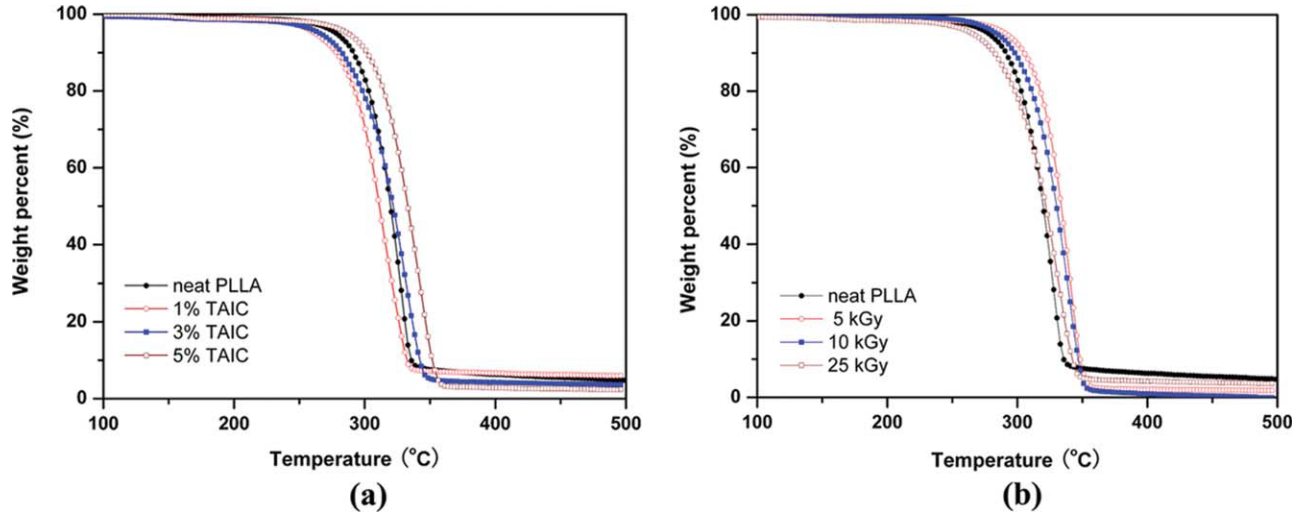

FIGURE 6. TGA curves of (a) PLLA/TAIC nanofibers containing different TAIC contents irradiated at 25 kGy. (b) PLLA/3% TAIC nanofibers crosslinked at different radiation doses. [Color figure can be viewed in the online issue, which is available at wileyonlinelibrary.com.]

TABLE I. TGA Results for Neat PLLA Nanofibers and Crosslinked PLLA/TAIC nanofibers

TAIC Content (%)	Radiation Dose (kGy)	T_{onset} (°C)	$T_{0.1}$ (°C)	$T_{0.5}$ (°C)	$\Delta T_{0.5}$ (°C)
0	0	295	290	320	–
1	25	288	278	312	−8
3	5	317	304	334	12
	10	298	298	329	9
	25	299	282	321	1
5	25	307	300	333	13

$T_{0.1}$ = temperature at 10% mass loss; $T_{0.5}$ = temperature at 50% mass loss; $\Delta T_{0.5}$ = temperature difference at 50% mass loss between the crosslinked sample and the neat PLLA.

crosslinked samples suggested that the molecular chains were crosslinked in the amorphous state. The high crosslinking density of PLLA restrains the molecular motion for crystallization, therefore reduces the melting temperature of the crosslinked samples.[16,17]

Figure 6 shows the thermogravimetric analysis (TGA) curves for crosslinked PLLA with different TAIC contents and different radiation doses. The thermal decomposition profiles of all the samples display a one-stage decomposition pattern during the thermal decomposition. As shown in Figure 6(a) which illustrates the effects of TAIC contents on the thermal stability of crosslinked PLLA samples at 25 kGy radiation dose, the onset degradation temperature (T_{onset}) of the neat PLLA sample was 295°C, whereas crosslinked PLLA/TAIC samples were 288, 299, and 307°C, respectively. Besides the sample with 1% TAIC content, other crosslinked samples achieved an improved thermal stability. Figure 6(b) illustrates the effects of the radiation dose on the thermal stability of crosslinked PLLA/3% TAIC samples, all the crosslinked scaffolds showed an increased T_{onset} as

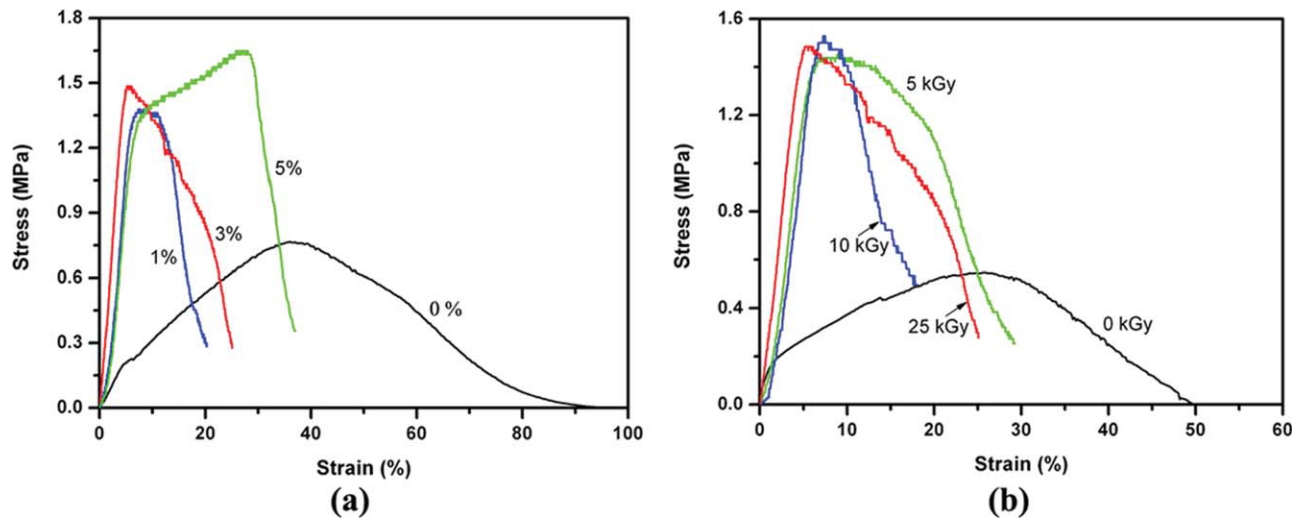

FIGURE 7. Typical ensile stress–strain curves of (a) PLLA/TAIC nanofibers containing different TAIC contents irradiated at 25 kGy, (b) PLLA/3% TAIC nanofibers crosslinked at different radiation doses. [Color figure can be viewed in the online issue, which is available at wileyonlinelibrary.com.]

TABLE II. Tensile Mechanical Properties of Neat PLLA Nanofibers and Crosslinked PLLA/TAIC Nanofibers

TAIC Content (%)	Radiation Dose (kGy)	Tensile Strength (MPa)	Elongation at Break (%)	Young's Modulus (MPa)
0	0	0.76 ± 0.06	88.45 ± 12.24	2.10 ± 0.35
1	0	0.72 ± 0.13	78.58 ± 10.35	2.38 ± 0.23
	5	0.91 ± 0.16	34.12 ± 16.13	20.92 ± 6.03
	10	0.87 ± 0.24	25.35 ± 4.82	16.40 ± 3.48
	25	1.39 ± 0.26	20.45 ± 4.01	33.93 ± 5.72
3	0	0.53 ± 0.11	54.64 ± 7.92	2.59 ± 0.10
	5	1.37 ± 0.41	28.29 ± 5.34	35.67 ± 8.04
	10	1.27 ± 0.19	20.80 ± 5.83	26.65 ± 8.54
	25	1.50 ± 0.25	20.78 ± 4.52	31.71 ± 8.61
5	0	0.74 ± 0.13	76.81 ± 10.94	2.65 ± 0.99
	5	1.12 ± 0.12	35.42 ± 9.36	21.93 ± 3.39
	10	1.84 ± 0.20	46.26 ± 8.74	30.98 ± 5.03
	25	1.67 ± 0.33	40.59 ± 7.27	25.97 ± 8.44

compared to the neat PLLA sample, but the T_{onset} decreased with increasing of the radiation doses.

To further confirm the effect of the crosslinking conditions on the thermal stability of crosslinked samples, the characteristic thermal degradation temperatures, including $T_{0.1}$ and $T_{0.5}$, defined as the temperature at which 10 and 50% mass loss occurs respectively, are summarized in Table I. It can be found that $T_{0.1}$ and $T_{0.5}$ of crosslinked samples were higher than that of neat PLLA at the appropriate radiation doses, indicating improvement of thermal stability of PLLA. However, too high radiation doses have an adverse effect on the thermal stability of crosslinked samples, especially in the case of lower TAIC content. For example, for PLLA/1% TAIC sample irradiated at 25 kGy, all the characteristic thermal degradation temperatures including T_{onset}, $T_{0.1}$, and $T_{0.5}$ were lower than those of neat PLLA sample. Furthermore, for PLLA/ 3% TAIC samples, high radiation dose of 25 kGy resulted in a relatively poor thermal stability of PLLA with decrease of all characteristic thermal degradation temperatures. This suggests that although high dosage of gamma irradiation facilitates the formation of crosslinking network, it might damage the PLLA chain and induce the thermal degradation of PLLA, resulting in poor thermal stability of the crosslinked PLLA.

Mechanical properties

Figure 7 shows the typical tensile stress–strain curve of crosslinked PLLA with different TAIC contents and different radiation doses. The tensile strength, elongation at break and Young's modulus are summarized in Table II. It can be found from Figure 7(a) and Table II that the increasing of TAIC contents increased the tensile strength but decreased the Young's modulus and elongation at break at 25 kGy radiation dose. Moreover, a sharp increase in Young's modulus and decrease in elongation at break were observed in all the crosslinked samples. For example, the average Young's modulus and elongation at break for PLLA/1% TAIC crosslinked sample at 25 kGy were 33.93 MPa and 20.45% as compared to 2.10 MPa and 88.45% for unirradiated neat PLLA sample. The results revealed that the crosslinked PLLA sample is stiffer than its uncrosslinked counterpart because of the formation of new bonds among different PLLA chains, and the crosslinked samples become stronger and more brittle with increasing TAIC content. This increase can be attributed to higher crosslinking density in the crosslinked samples with higher TAIC content, which possesses a higher double bond concentration for crosslinking of PLLA.[21]

The influence of radiation dose on the stress and strain curves for irradiated PLLA/3% TAIC samples is illustrated in Figure 7(b). All the irradiated samples exhibited enhanced mechanical properties such as increased strength and Young's modulus as compared to unirradiated sample. Combining with Table II, we can conclude that the tensile strength and Young's modulus of samples increased when the radiation dose was increased, whereas the elongation at break reduced with the increasing radiation dose. It is well known that the double bonds in TAIC can be easily broken under radiation to produce radicals and then combine with polymer radicals to form the crosslinking structure.[16] The mechanical properties of crosslinked polymers are strongly dependent on the crosslinking density and chemical structure of the crosslinker introduced. The higher radiation dose may facilitate a more stable crosslinking network, which restricts the mobility of the polymer chains and thus decreases elongation at break of the crosslinked films, but increases the tensile strength and Young's modulus of samples.

Figure 8 shows dynamic mechanical properties including the storage modulus (E') and tan δ of crosslinked PLLA samples irradiated with different TAIC contents and different radiation doses, respectively. For neat PLLA, the curve of storage modulus demonstrated that PLLA exhibited glassy, glass-transition, crystallization, rubbery and liquid-flow behaviors; whereas the peak of tan δ indicated the T_g of neat PLLA nanofibers is around 78°C. All the crosslinked samples did not exhibit crystallization behavior but became more stable than neat PLLA at high temperature, and their T_g values increased with the increase of TAIC contents and radiation doses. The results demonstrated that the

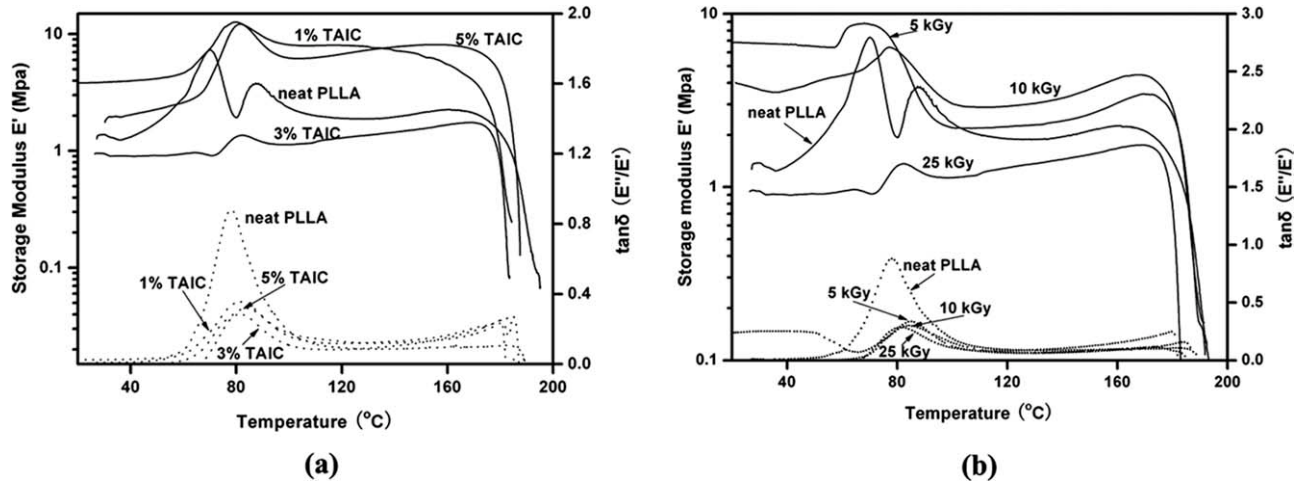

FIGURE 8. Storage modulus (E') and tan δ of (a) PLLA/TAIC nanofibers containing different TAIC contents irradiated at 25 kGy, (b) PLLA/3% TAIC nanofibers crosslinked at different radiation doses.

mechanical properties and thermal stability were improved by radiation-induced crosslinking with TAIC.

Biodegradability

Figure 9 shows enzymatic degradation curves of neat PLLA and PLLA/3% TAIC crosslinked at different radiation doses. All the samples, except the control sample which was hardly degraded in a buffer solution without enzyme, exhibited a linear relation between the weight loss and the degradation time. The weight loss of neat PLLA sample incubated with proteinase K for 8 days was about 15.6 mg cm^{-2}, whereas those of the crosslinked samples were obviously decreased at the same duration, implying that the formed crosslinking network by irradiation restricted the absorption of the enzyme into the polymer gels, and thus delayed the degradation of crosslinked samples. Generally, high radiation dose facilitates the formation of more stable crosslinking network and results in a low degradation rate.[22] In our case, however, the crosslinked sample irradiated at 10 kGy exhibited the minimum weight loss, whereas the sample irradiated at 25 kGy achieved a higher degradation rate. This can be explained by the fact that high dose radiation can induce chain scission within polymers, resulting in reduction of molecular weight and consequently increase of degradation rate.[23] Therefore, the radiation dose of 10 kGy was chosen for preparing the crosslinked PLLA samples for cell culture experiments.

Figure 10 shows SEM images of different degraded samples after 8 days incubation, the image of degraded neat PLLA sample with enzyme was not included since the sample was almost completely degraded within 8 days. The control sample still maintained its fibrous structure after 8 days incubation in buffer solution without enzyme, as shown in Figure 10(a). Meanwhile, all the crosslinked samples showed a swollen morphology with partial fibrous structure still containing, indicating that the crosslinked PLLA network is able to resist the cleavage of proteinase K.

Degradation behavior of a polymeric scaffold is a critical factor affecting the long-term success of a tissue-engineered cell/polymer construct. The degradation profiles may influence a wide range of biological processes such as cell growth, tissue regeneration, and host response.[24] PLLA is a semicrystalline polyster with high crystallinity and hydrophobicity, which makes it degrade very slowly both *in vitro* and *in vivo*. Enzymatic degradation has been considered as a rapid method to evaluate the degradation behavior of PLLA in a short term, although they are not completely responsible for the hydrolysis of polymers. However, it should be noted that the degrading activity of crosslinked PLLA fibers in physiological environment is markedly different from our present study; further studies need to be done to ascertain the *in vivo* degradation kinetics of this material before it can be used for practical applications in tissue engineering.

Cellular behavior

L929 mouse fibroblast cells were seeded and cultivated on the different crosslinked scaffolds to evaluate cellular behavior, and cells were also cultivated on the neat PLLA scaffold for comparison. Figure 11 show the proliferation of L929 fibroblast cells on the crosslinked PLLA/TAIC scaffolds with different TAIC contents (irradiated at 10 kGy) after seeding for 1, 3, 5, and 7 days. In general, cell proliferation on all the crosslinked scaffolds was higher that on neat PLLA scaffold, but no significant difference was found among all tested groups after 1, 3, and 5 days. However, a significant increase in cell proliferation was observed at day 7 for PLLA/3% TAIC scaffold compared with neat PLLA scaffold ($p < 0.05$).

Figure 12 shows SEM images of cultured cells on the neat PLLA and crosslinked scaffolds after seeding for 3 days. It can be seen that the fibroblast cells were well grown and spread on all the tested scaffolds, and the number of cells that were cultured on the crosslinked scaffolds

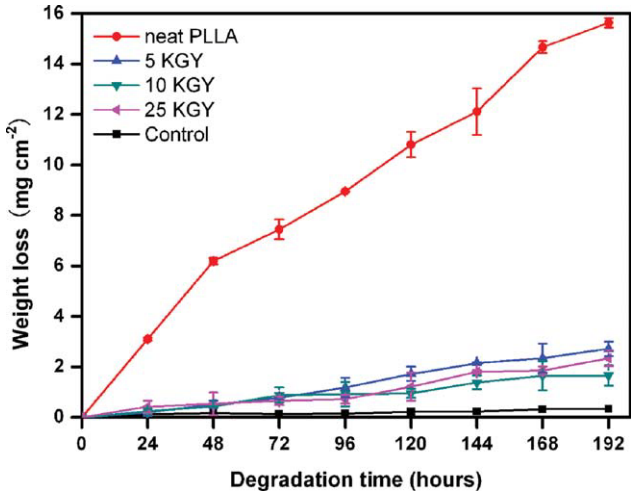

FIGURE 9. Enzymatic degradation curves of neat PLLA and PLLA/3% TAIC crosslinked at different radiation doses. PLLA nanofibers immerged in buffer without enzyme set as control. [Color figure can be viewed in the online issue, which is available at wileyonlinelibrary.com.]

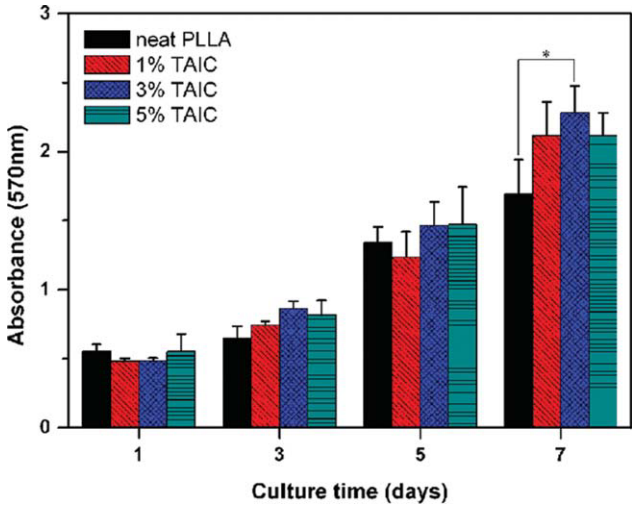

FIGURE 11. Proliferation of L929 fibroblast cells on the crosslinked PLLA/TAIC scaffolds with different TAIC contents (irradiated at 10 kGy) after seeding for 1, 3, 5, and 7 days. Data were expressed as mean ± SD ($n = 3$). Significant difference between groups is indicated ($*p < 0.05$). [Color figure can be viewed in the online issue, which is available at wileyonlinelibrary.com.]

appeared to be greater than that on the neat PLLA scaffold, which are in agreement with the results obtained from the cell proliferation assays. The results from cell proliferation assays suggested that the radiation crosslinking with TAIC did not induce any cytotoxic activity on the seeded fibroblast cells under our experimental conditions. Moreover, the crosslinked scaffolds possess the improved dimensional stability and mechanical strength, which is beneficial for their application in tissue engineering and other biomedical areas. However, more work should be done to further evaluate the biocompatibility and biodegradability of crosslinked scaffolds before they can be used in tissue engineering.

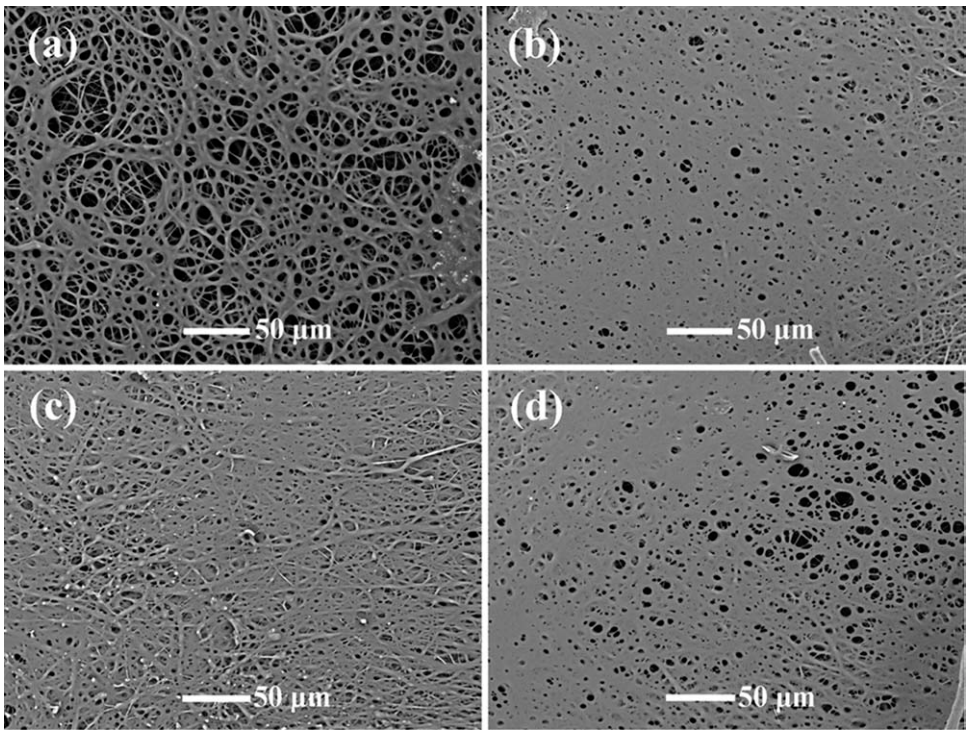

FIGURE 10. SEM images of different degraded samples after 8 days incubation. (a) PLLA nanofibers immerged in buffer without enzyme, and enzymatic degradation of PLLA/3% TAIC nanofibers irradiated at (b) 5 kGy, (c) 10 kGy, (d) 25 kGy after 8 days incubation in buffer containing proteinase K.

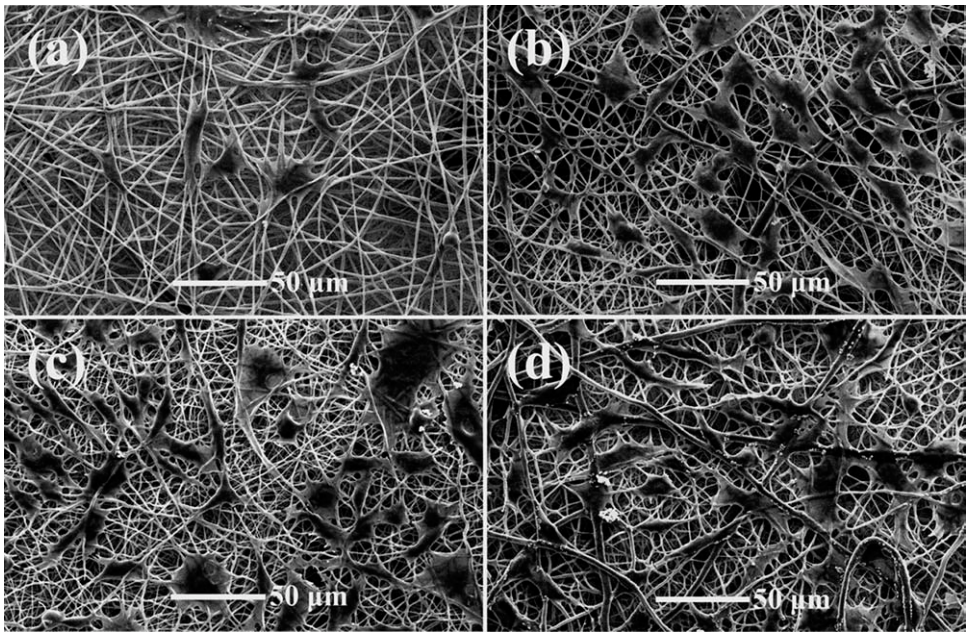

FIGURE 12. SEM images of L929 cells grown on (a) neat PLLA nanofibers and crosslinked PLLA/TAIC nanofibers irradiated at 10 kGy with various concentration of TAIC (b) 1%, (c) 3%, (d) 5% after culture for 3 days.

CONCLUSIONS

The PLLA/TAIC composite nanofibers were fabricated by electrospinning and subsequently crosslinked by gamma irradiation with different radiation dose. The efficient crosslinking networks can be generated in the crosslinked samples when the TAIC content is higher than 3%. The thermal stability and tensile mechanical properties were significantly increased by radiation crosslinking at higher irradiation dose of 10 and 25 kGy. However, radiation dose at 25 kGy exert an adverse effect on the thermal stability of crosslinked samples due to thermal degradation induced by irradiation, the crosslinked samples irradiated at 10 kGy exhibited the best enzymatic degradation. The *in vitro* results also revealed that the crosslinked PLLA/TAIC composite nanofibers did not induce cytotoxic effects and suitable for cell growth. Therefore, the crosslinked PLLA nanofibers are one of the promising materials for tissue engineering applications.

ACKNOWLEDGMENTS

The authors gratefully acknowledge Dr. Yanfeng Zhang (University of Science and Technology of China) for his assistance with gamma irradiation studies.

REFERENCES

1. Langer R, Vacanti JP. Tissue engineering. Science 1993;260: 920–926.
2. Lutolf MP, Hubbell JA. Synthetic biomaterials as instructive extracellular microenvironments for morphogenesis in tissue engineering. Nat Biotechnol 2005;23:47–55.
3. Langer R, Tirrell DA. Designing materials for biology and medicine. Nature 2004;428:487–492.
4. Zhang SG. Fabrication of novel biomaterials through molecular self-assembly. Nat Biotechnol 2003;21:1171–1178.
5. Ma PX. Biomimetic materials for tissue engineering. Adv Drug Deliv Rev 2008;60:184–198.
6. Li WJ, Laurencin CT, Caterson EJ, Tuan RS, Ko FK. Electrospun nanofibrous structure: A novel scaffold for tissue engineering. J Biomed Mater Res 2002;60:613–621.
7. Pham QP, Sharma U, Mikos AG. Electrospinning of polymeric nanofibers for tissue engineering applications: A review. Tissue Eng 2006;12:1197–1211.
8. Liu XH, Ma PX. The nanofibrous architecture of poly(L-lactic acid)-based functional copolymers. Biomaterials 2010;31:259–269.
9. He CL, Huang ZM, Han XJ, Liu L, Zhang HS, Chen LS. Coaxial electrospun poly(L-lactic acid) ultrafine fibers for sustained drug delivery. J Macromol Sci B 2006;45:515–524.
10. He CL, Huang ZM, Han XJ. Fabrication of drug-loaded electrospun aligned fibrous threads for suture applications. J Biomed Mater Res 2009;89A:80–95.
11. He CL, Xiao GY, Jin XB, Sun CH, Ma PX. Electrodeposition on nanofibrous polymer scaffolds: Rapid mineralization, tunable calcium phosphate composition and topography. Adv Funct Mater 2010;20:3568–3576.
12. Lee JH, Park TG, Park HS, Lee DS, Lee YK, Yoon SC, Nam JD. Thermal and mechanical characteristics of poly(L-lactic acid) nanocomposite scaffold. Biomaterials 2003;24:2773–2778.
13. Yang SL, Wu ZH, Yang W, Yang MB. Thermal and mechanical properties of chemical crosslinked polylactide (PLA). Polym Test 2008;27:957–963.
14. Mitomo H, Kaneda A, Quynh TM, Nagasawa N, Yoshii F. Improvement of heat stability of poly(L-lactic acid) by radiation-induced crosslinking. Polymer 2005;46:4695–4703.
15. Zhang XW, Kotaki M, Okubayashi S, Sukigara S. Effect of electron beam irradiation on the structure and properties of electrospun PLLA and PLLA/PDLA blend nanofibers. Acta Biomater 2010;6: 123–129.
16. Jin FZ, Hyon SH, Iwata H, Tsutsumi S. Crosslinking of poly(L-lactide) by gamma-irradiation. Macromol Rapid Commun 2002;23: 909–912.
17. Quynh TM, Mitomo H, Nagasawa N, Wada Y, Yoshii F, Tamada M. Properties of crosslinked polylactides (PLLA and PDLA) by radiation and its biodegradability. Eur Polym J 2007;43: 1779–1785.
18. Huang ZM, He CL, Yang AZ, Zhang YZ, Hang XJ, Yin JL, Wu Q. Encapsulating drugs in biodegradable ultrafine fibers through co-axial electrospinning. J Biomed Mater Res 2006;77A: 169–179.

19. Huang ZM, Zhang YZ, Kotaki M, Ramakrishna S. A review on polymer nanofibers by electrospinning and their applications in nanocomposites. Compos Sci Technol 2003;63:2223–2253.
20. Nugroho P, Mitomo H, Yoshii F, Kume T. Degradation of poly(L-lactic acid) by gamma-irradiation. Polym Degrad Stab 2001;72: 337–343.
21. Quynh TM, Mitomo H, Zhao L, Tamada M. Properties of a poly(L-lactic acid)/poly(D-lactic acid) stereocomplex and the stereocomplex crosslinked with triallyl Isocyanurate by irradiation. J Appl Polym Sci 2008;110:2358–2365.
22. Quynh TM, Mitomo H, Yoneyama M, Hien NQ. Properties of radiation-induced crosslinking stereocomplexes derived from poly(L-Lactide) and different poly(D-Lactide). Polymer Eng Sci 2009;49: 970–976.
23. Cairns ML, Dickson GR, Orr JF, Farrar D, Hawkins K, Buchanan FJ. Electron-beam treatment of poly(lactic acid) to control degradation profiles. Polym Degrad Stab 2011;96:76–83.
24. Lu LC, Peter SJ, Lyman MD, Lai HL, Leite SM, Tamada JA, Vacanti JP, Langer R, Mikos AG. In vitro degradation of porous poly(L-lactic acid) foams. Biomaterials 2000;21:1595–1605.